Catalysis Science & Technology

RSCPublishing

PAPER

View Article Online
View Journal

Preparation of L-phenylalaninol with high *ee* selectivity by catalytic hydrogenation of L-phenylalaninate over $Cu/ZnO/Al_2O_3$ catalyst

Cite this: DOI: 10.1039/c2cy20763j

Chunyou Gao,[a] Xiuzheng Xiao,[a] Dongsen Mao[a] and Guanzhong Lu*[ab]

Received 8th November 2012,
Accepted 11th December 2012

DOI: 10.1039/c2cy20763j

www.rsc.org/catalysis

The $Cu/ZnO/Al_2O_3$ catalyst for hydrogenation of L-phenylalaninate to L-phenylalaninol was prepared by a co-precipitation method, and characterized by XRD, low-temperature N_2 adsorption, H_2-TPR, N_2O chemisorption and ICP-AES. The results show that the physicochemical properties of the catalyst are greatly affected by the ZnO amount, and that the exposed copper surface area, dispersion of CuO and BET surface area of the $Cu/ZnO/Al_2O_3$ catalyst (Cu/Zn/Al = 1.0 : 0.3 : 1.0) reach the largest. The chemoselectivity of L-phenylalaninol is changed with ZnO amount in the $Cu/ZnO/Al_2O_3$ catalyst, and when Cu/Zn/Al = 1.0 : 0.3 : 1.0, the catalyst exhibits higher catalytic performance and chemoselectivity to L-phenylalaninol. Furthermore, the effect of temperature, pressure, reaction time and the molar ratio of catalyst to ester on the catalytic hydrogenation of L-phenylalaninate were investigated. When the catalytic hydrogenation of L-phenylalaninate was operated at 110 °C and 4 MPa of H_2 for 5 h, the yield of L-phenylalaninol can reach 69.2 %, and its *ee* selectivity is 99.84 %.

1 Introduction

The formation of chiral amino alcohols, especially L-phenylalaninol, has become the subject of considerable interest because of their importance in asymmetric synthesis, peptide and pharmaceutical chemistry, resolution of racemic mixtures, synthesis of insecticidal compounds, *etc.*[1–10]

L-Phenylalaninol has often been prepared by reducing the corresponding L-phenylalanine or esters. In most cases, metal hydrides were used as reducing agents, which are reactive at low temperature thereby guaranteeing the integrity of the stereogenic center. It was reported that $LiAlH_4$,[11,12] $LiAlH_4$-THF,[13] BH_3,[14] $NaBH_4$ ($NaBH_4$/LiCl, $NaBH_4/TiCl_4$, $NaBH_4/CeCl_3$, $NaBH_4$-I_2-THF, $NaBH_4$/Cyanuric chloride, $NaBH_4/I_2$),[15–20] KBH_4-$CaCl_2$,[21] $Zn(BH_4)_2$,[22] $LiBH_4$/DCC,[23] and various Lewis base catalysts[24] have been employed for the reduction of L-phenylalanine or esters to obtain L-phenylalaninol. Even though these reactions can be carried out at room temperature on a 100–150 g scale, the costs and the large amount of waste render this methodology less attractive for technical applications.[25]

Therefore, another approach of catalytic hydrogenation is obviously more attractive. However, carboxylic acids and esters are the least reactive functional groups for classical hydrogenation catalysts, and a reaction temperature of >200 °C is usually needed for efficient transformation, which will cause the racemization of products.[26]

The industrial potential of amino alcohols has driven the research of catalysts for the effective hydrogenation of amino acids or esters for a very long time. From the earliest reports by Ovakimian, Kuna and Levene, Raney nickel was used as the catalyst for the hydrogenation of esters of certain amino acids to amino alcohols at 35–100 °C.[27] Then, 10 years ago, Nishimura's catalyst (mixed Pt–Rh oxide of 45.9% Rh and 19.9% Pt) was reported to catalyze the hydrogenation of amino esters to the corresponding amino alcohols at 25 °C under 10 MPa hydrogen pressure without racemization, while the phenyl group was catalytically hydrogenated to a cyclohexyl group, simultaneously.[26] Recently, a ruthenium complex was found to catalyze the hydrogen reduction of optically active esters to the corresponding chiral alcohols without any loss of optical purities. A variety of optically active esters can be reduced to the corresponding alcohols in excellent yield without loss of their optical purity or causing undesirable side reactions, except for amino esters.[28]

As is well-known, copper-containing catalysts are widely used for the hydrogenation of esters to alcohols, because they allow the selective hydrogenation of carbon–oxygen bonds and

[a] *Research Institute of Applied Catalysis, School of Chemical and Environmental Engineering, Shanghai Institute of Technology, Shanghai 200235, P. R. China. E-mail: gzhlu@ecust.edu.cn; Fax: (+86)-21-64253824*

[b] *Key Laboratory for Advanced Materials and Research Institute of Industrial catalysis, East China University of Science and Technology, Shanghai 200237, P. R. China*

are relatively inactive for carbon–carbon bond hydrogenolysis.[29] Among them, $Cu/ZnO/Al_2O_3$ catalysts are typical catalysts, and are employed in the synthesis of methanol,[30–33] the synthesis of *N*-ethylethylenediamine,[34] gas phase hydrogenolysis[35] and hydrogenolysis of glycerol to propylene glycol.[36] However, the effect of a ZnO promoter in copper catalysts is a matter of controversy in the hydrogenation of esters to alcohols. Some research works suggest that Zn can increase electron density on copper and can store or activate hydrogen.[37–39] It was reported that in the Cu–ZnO mixed oxide, highly active and epitaxially-bound metallic copper platelets can be formed after a reduction of catalyst.[40–42] Kawamura *et al.* thought that the presence of Zn can increase the dispersion of Cu particles.[43] However, though much work has been done on copper catalysts for the hydrogenation of fatty esters to alcohols, no detailed research works have been reported on a copper catalyst for the hydrogenation of amino acids or esters to corresponding alcohols.

In this paper, we have developed a $Cu/ZnO/Al_2O_3$ catalyst for the hydrogenation of methyl L-phenylalaninate to methyl L-phenylalaninol under mild reaction conditions, in which the catalyst is very cheap and highly effective. The $Cu/ZnO/Al_2O_3$ catalyst was prepared by the co-precipitation method and exhibits higher activity and selectivity for methyl L-phenylalaninol synthesis by L-phenylalaninate hydrogenation, which may be useful for commercial applications of the catalyst in the hydrogenation of L-phenylalaninate to methyl L-phenylalaninol. This reaction formula is described as follows:

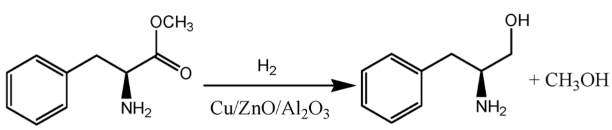

2 Experimental

2.1 Catalyst preparation

The $Cu/ZnO/Al_2O_3$ catalysts were prepared by the co-precipitation method. The starting materials were $Cu(NO_3)_2{\cdot}3H_2O$, $Zn(NO_3)_2{\cdot}3H_2O$ and $Al(NO_3)_3{\cdot}3H_2O$ (A.R., Sinopharm Chemical Reagent Ltd.) which were dissolved in de-ionized water to form 1 mol L^{-1} aqueous solution. Then, 10% ammonia aqueous solution was added into 1 mol L^{-1} $Al(NO_3)_3$ solution until pH 8.0, and 0.5 mol L^{-1} Na_2CO_3 solution was added into a mixed solution of 1 mol L^{-1} $Cu(NO_3)_2$ and 1 mol L^{-1} $Zn(NO_3)_2$ until pH 8.0, in which 10% ammonia aqueous solution and Na_2CO_3 solution were used as a precipitating agent. After two as-prepared solutions were mixed under stirring, this synthesis solution was aged for 5 h at 70 °C under stirring in an oil bath, and then it was cooled to room temperature at static conditions and kept for 2 h. The precipitate was filtrated, and washed with de-ionized water and ethanol until the filtrate was neutral. After being dried in air at 120 °C for 24 h, the catalysts were calcined at 450 °C for 4 h, and pressed and crushed to 0.45–0.85 mm (20–40 mesh). The resulting $Cu/ZnO/Al_2O_3$ catalysts with different Zn amounts were termed as C0, C1, C3, C4, C5 and C7, respectively. The compositions of $Cu/ZnO/Al_2O_3$ catalysts are listed in Table 1.

Table 1 The molar compositions of Cu, Zn and Al in $Cu/ZnO/Al_2O_3$ catalysts

	In synthesis gel			In solid catalyst[a]		
Catalyst	Cu	Zn	Al	Cu	Zn	Al
C0	1	0	1	1.07 (49.9)[b]	0	1
C1	1	0.1	1	1.08 (47.3)	0.10	1
C3	1	0.3	1	1.03 (41.2)	0.32	1
C4	1	0.4	1	1.03 (38.8)	0.44	1
C5	1	0.5	1	1.07 (37.6)	0.55	1
C7	1	0.7	1	1.05 (34.4)	0.73	1

[a] Analyzed by ICP. [b] The value in brackets is Cu amount (wt%) in the catalyst.

2.2 Catalyst characterization

The compositions of Cu, Zn and Al in the $Cu/ZnO/Al_2O_3$ catalysts were analyzed by inductively coupled plasma-atomic emission spectroscopy (ICP-AES, optical emission spectrometer, Optima 7000 DV). The surface areas of the catalysts were measured by N_2 adsorption at −196 °C on a Micrometrics ASAP 2020 apparatus and calculated by the Brumauer–Emmett–Teller (BET) method.

The powder X-ray diffraction (XRD) patterns of the catalysts were recorded on a PANalytical PW 3040/60 X'Pert PRO diffractometer with Ni-filtered CuKα radiation and operated at 40 kV and 40 mA. The average crystallite sizes of the catalysts were calculated based on diffraction peak broadening by the Scherrer equation.

H_2-temperature-programmed reduction (H_2-TPR) was performed on a flow system equipped with a thermal conductivity detector (TCD) as follows: 50 mg catalyst was used and pretreated at 350 °C for 1 h under N_2 flow of 50 mL min^{-1}. After it was cooled to room temperature under N_2, it was flushed by 10% H_2/N_2 of 50 mL min^{-1} instead of N_2, and TPR of the sample was run from room temperature to 500 °C at 10 °C min^{-1}. Effluent gas was dried by powder KOH and consumption of hydrogen was analyzed by TCD. The amount of hydrogen consumption was calibrated by using a known amount of CuO,[44] and denoted as *X*. The amount of surface metallic copper sites was determined by dissociative N_2O adsorption at 50 °C,[44,45] and the experimental procedure was as follows: the catalyst was first reduced in the TPR procedure described above by 10% H_2/N_2 (50 mL min^{-1}) from room temperature to 500 °C. Then the catalyst bed was purged with N_2 (50 mL min^{-1}), cooled to 50 °C, and then oxidized in 2% N_2O/He (50 mL min^{-1}) at 50 °C for 0.5 h. Finally, the catalyst was flushed with N_2 to remove any N_2O oxidant and cooled to room temperature to begin the second TPR run. Hydrogen consumption in the second TPR was denoted as *Y*. The dispersion of Cu and exposed Cu surface area were calculated by the following equations:

All copper atoms were reduced in the first TPR:

$$CuO + H_2 \rightarrow Cu + H_2O, \text{ hydrogen consumption} = X$$

Surface copper oxidized by N_2O at 50 °C to Cu_2O was then reduced in the second TPR:

$$Cu_2O + H_2 \rightarrow 2Cu + H_2O, \text{ hydrogen consumption} = Y$$

The dispersion of Cu (D_{Cu}) and the exposed Cu surface area (S_{Cu}) were calculated as follows:

$$D_{Cu} = (2 \times Y/X) \times 100\%$$

$$S_{Cu} = 2 \times Y \times N_{AV}/(X \times M_{Cu} \times (1.4 \times 10^{19})) = 1353 \times Y/X\,(m^2{}_{Cu}\,g_{Cu}{}^{-1})$$

where N_{AV} = Avogadro's constant, M_{Cu} = relative atomic mass (63.456 g mol^{-1}), and 1.4×10^{19} is inferred from the equal abundance of an average copper surface atom area of 0.0711 nm^2 (equivalent to 1.4×10^{19} copper atoms per square meter).

2.3 Testing of catalyst performance

The performance of catalyst for methyl L-phenylalaninate hydrogenation was tested in a 0.5 L stainless steel autoclave under stirring at a speed of 500 rpm. Prior to the catalytic activity measurement, 1 g (20–40 mesh) catalyst in the stainless steel autoclave was reduced in H_2 (>99.999%) at 1 MPa and 250 °C for 4 h, then the autoclave was cooled to room temperature under H_2 and methyl L-phenylalaninate diluted in ethanol (>99.999%) was introduced. The typical reaction conditions are 80 °C and 3 MPa of H_2 for 5 h, and the mass ratio of catalyst/L-phenylalaninate (Cat./L-p) is 1. Reactants and products were analyzed by high performance liquid chromatography (HPLC) equipped with an ultraviolet detector and fitted with a column (eclipse XDB-C18, 150 × 4.6 mm, 5 μm column P/N 993967-902). The operating conditions of HPLC were such that the mobile phase was 0.05 mol L^{-1} ammonium acetate (pH = 5)/methanol (30 : 70) of 0.6 mL min^{-1}, detection wavelength of 254 nm, injection volume of 6 μL, and column temperature of 20 °C. The conversion of methyl phenylalaninate (X) and chemoselectivity to methyl L-phenylalaninol (S) were calculated as follows:

X (%) = (molar amount of L-phenylalaninate converted/total molar amount of L-phenylalaninate in the feed) × 100

S (%) = (molar amount of L-phenylalaninol formed/total molar amount of L-phenylalaninate in the feed) × 100

Yield of L-phenylalaninol (%) = $X \times S$

3 Results and discussion

3.1 Textural and structural properties of catalysts

In preparation of $Cu/ZnO/Al_2O_3$ catalysts, the molar compositions of Cu, Zn and Al in synthesis solutions and prepared copper-based catalysts are listed in Table 1. It can be seen that the compositions of Cu, Zn and Al in $Cu/ZnO/Al_2O_3$ catalysts are similar to those in synthesis solutions.

The XRD patterns of the $Cu/ZnO/Al_2O_3$ catalysts are shown in Fig. 1. It can be seen that there are no diffraction peaks of Al_2O_3, which shows that any Al_2O_3 in the $Cu/ZnO/Al_2O_3$ catalysts is amorphous or highly-dispersed in both the fresh and reduced $Cu/ZnO/Al_2O_3$ catalysts. In the XRD patterns (Fig. 1A) of fresh catalysts, the characteristic diffraction peaks of CuO can be observed at 2θ = 35.56, 38.77, 48.66, 53.74, 58.29, 61.53, 66.07 and 68.19° (PDF 48-1548). For the reduced catalysts, the peaks of CuO disappear and peaks of metallic copper can be observed at 2θ = 43.24 and 50.33° (PDF 04-0836) (Fig. 1B), indicating that CuO has been reduced to Cu^0. Similar XRD

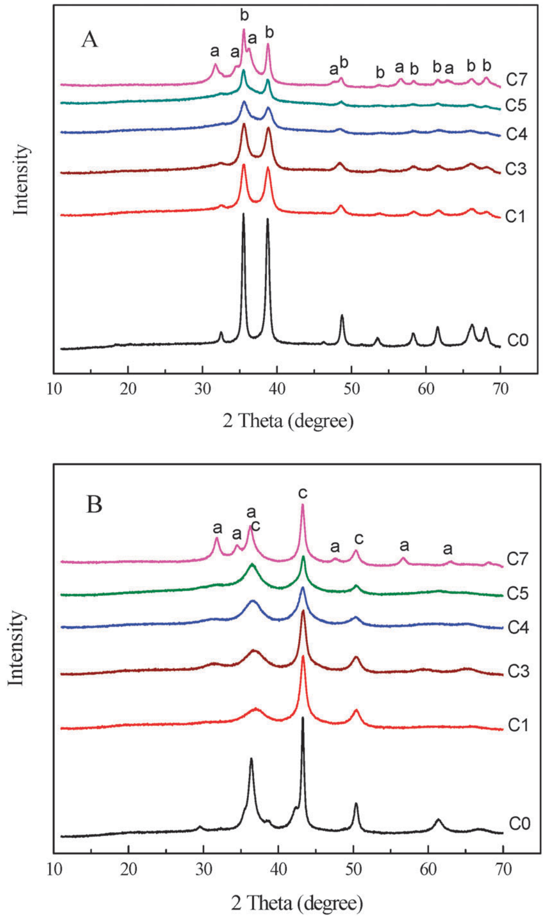

Fig. 1 XRD patterns of (A) fresh and (B) reduced $Cu/ZnO/Al_2O_3$ and Cu/Al_2O_3 catalysts. (a = ZnO; b = CuO; c = Cu^0).

results have been reported by Y.H. Feng *et al.* for $Cu/ZnO/MO_x$ (MO_x = Al_2O_3, TiO_2, and ZrO_2) catalysts.[35] In the XRD patterns of both fresh and reduced catalysts, the characteristic peaks of ZnO appear at 2θ = 31.71, 33.95, 36.26, 47.72, 56.71 and 62.83° (PDF 36-1451) when the ZnO amount reaches Zn/Cu = 0.7 (mol), which shows that ZnO in $Cu/ZnO/Al_2O_3$ catalysts cannot be reduced under such reduction conditions. When Zn/Cu <0.7 (mol) in the catalyst, such as the C5 catalyst, no diffraction peaks of ZnO can be observed, which should be ascribed to its high dispersion in the catalyst.

The average crystallite size of Cu^0 in the reduced catalyst was calculated based on the XRD patterns by the Scherrer equation and their results are shown in Table 2. We can find that the crystallite size of Cu^0 varies with the ZnO amount. When the Zn/Cu ratio is <0.7 (mol) in the catalyst, the average crystallite size of Cu^0 in the reduced catalyst is decreased with an increase in the Zn amount, in which the diffraction peaks of ZnO cannot be observed. For the reduced C7 catalyst with Zn/Cu = 0.7 (mol), the diffraction peaks of ZnO can be obviously observed. The crystallite size of Cu^0 is decreased conversely with an increase in the Zn amount. This is attributed to the separation of ZnO and CuO phases in the $Cu/ZnO/Al_2O_3$ catalyst when the Zn amount is higher (Fig. 1A).

Table 2 BET surface areas (S_{BET}), metallic copper surface areas (S_{Cu}), dispersions of Cu (D_{Cu}) and Cu crystallite sizes (d) of Cu/ZnO/Al_2O_3 catalysts

Catalyst	S_{BET} ($m^2\ g^{-1}$)	S_{Cu} ($m^2\ g_{Cu}^{-1}$)	S_{Cu} ($m^2\ g_{Cat}^{-1}$)	D_{Cu} (%)	d (nm)[a]
C0	112	189	93.3	27.7	16.8
C1	150	197	93.2	29.1	7.37
C3	160	275	113	40.7	6.93
C4	149	233	90.4	34.5	4.72
C5	77	97.4	36.6	14.4	3.52
C7	77	100	34.4	14.8	6.55

[a] It is the Cu average crystallite size in reduced catalyst and calculated based on XRD patterns by Scherrer equation.

The BET surface areas of Cu/ZnO/Al_2O_3 catalysts derived from nitrogen physisorption are listed in Table 2. The results show that with an increase in the ZnO amount, the BET surface areas of catalysts firstly increase and then decrease. The minimum surface area was obtained for C5 and C7, which is 77 $m^2\ g^{-1}$, while C3 exhibits a maximum surface area of 160 $m^2\ g^{-1}$.

The metallic copper surface area (S_{Cu}) of the catalyst was investigated by means of the reactive N_2O adsorption technique, and the results are shown in Table 2. We can find that the variation trend of metallic copper surface area with an increase in the ZnO amount is similar to that of the BET surface area. The minimum surface area of metallic copper was obtained for C5 and C7, which is 34–37 $m^2\ g_{cat}^{-1}$, and C3 has the maximum surface area of metallic copper (113 $m^2\ g_{cat}^{-1}$). It is well-known that the metallic copper surface area reflects the dispersion of Cu in the catalyst;[46] that is to say, the smaller the metallic copper surface area, the lower the dispersion of Cu. Therefore C3 possesses the highest dispersion of Cu (D_{Cu}) and C5 and C7 possess the lowest dispersions of Cu, which is in agreement with the data shown in Table 2.

According to the above results, we can see that the Cu dispersion is correlated with the loading amount of ZnO in the Cu/ZnO/Al_2O_3 catalyst. The interaction between ZnO promoter and Cu can increase the Cu dispersion, while ZnO has occupied the Cu sites on the catalyst surface, resulting in a decrease of the effective surface area of Cu. Therefore, we may surmise that when the loading amount of ZnO is lower (Zn/Cu $\leq$0.3), the interaction between ZnO and Cu is stronger, thus increasing the Cu dispersion, and when the loading amount of ZnO is higher (Zn/Cu $\geq$0.3), much more ZnO has occupied the Cu sites to make the effective surface area of Cu decrease.

3.2 The reduction properties of catalysts

The H_2-TPR technique was used to investigate the reduction behaviour of the Cu/ZnO/Al_2O_3 catalysts, and the results are shown in Fig. 2. The results show that the reduction profiles of all samples with different ZnO amounts exhibit a broad peak of H_2 consumption at 200–320 °C, in which the reduced peaks for C0, C5 and C7 can be disassembled to α and β peaks.

It is well-known that ZnO and Al_2O_3 cannot be reduced at below 500 °C, and that the presence of ZnO can promote the reduction of CuO by hydrogen spillover;[47] the α and β peaks are ascribed to the reduction of two kinds of Cu species or CuO

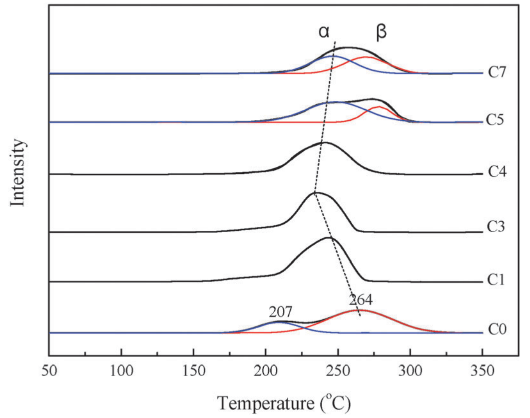

Fig. 2 H_2-TPR profiles of the Cu/ZnO/Al_2O_3 catalysts.

with different sizes. For the former, the reduction peak at lower temperature corresponds to $Cu^{2+} \rightarrow Cu^{+}$ and the peak at higher temperature corresponds to $Cu^{+} \rightarrow Cu^{0}$, and in the latter two reduction peaks corresponds to $Cu^{2+} \rightarrow Cu^{0}$, in which the peak at lower temperature is due to the reduction of highly-dispersed CuO and the peak at higher temperature is due to the reduction of bulk CuO.[48–50] In the TPR curve of C0 (CuO/Al_2O_3), there are two peaks and the α peak area is obviously unequal to that of the β peak. Thus, we can conclude that the α peak is ascribed to the reduction of highly-dispersed CuO on the catalyst surface and the β peak is ascribed to the reduction of bulk CuO in the catalyst. After adding ZnO with lower loading (C1, C3 and C4 samples), the two peaks in the TPR curve of C0 are overlapped, which indicates that the presence of ZnO makes CuO homogeneously disperse by forming a solid solution of Cu–Zn–O[49] that can be reduced at markedly lower temperatures compared to CuO.[51] Therefore, the reduction peak temperatures in C1, C3 and C4 catalysts are lower than that of the β peak in the C0 catalyst. With a further increase in the ZnO loading, a ZnO phase was formed in the Cu/ZnO/Al_2O_3 catalyst (as observed in the XRD spectra of C7 in Fig. 1). The interaction between Cu and ZnO weakened, resulting in decreasing the dispersion of CuO in the Cu/ZnO/Al_2O_3 catalyst and the presence of a β peak due to the reduction of bulk CuO.[46] Among the Cu/ZnO/Al_2O_3 catalysts, the C3 catalyst (Cu/Zn/Al = 1 : 0.3 : 1) shows the lowest temperature for the reduction peak. This confirms that the smaller the CuO particles, the lower the reduction temperature should be,[52] which is in good agreement with the highest surface area of Cu (S_{Cu}) and the surface dispersion of Cu (D_{cu}, Table 2).

The TPR results above prove that ZnO can promote the dispersion of copper oxide and enhance the reducibility of the copper phase; the low temperature peak (α peak) is attributed to the reduction of highly-dispersed CuO strongly interacting with ZnO, and the peak at higher temperature (β peak) is due to the reduction of bulk CuO.[46]

3.3 Catalytic performance of Cu/ZnO/Al_2O_3

3.3.1 Effect of the Zn content. The effect of ZnO content on the catalytic performance of the Cu/ZnO/Al_2O_3 catalyst for hydrogenation of methyl L-phenylalaninate was investigated

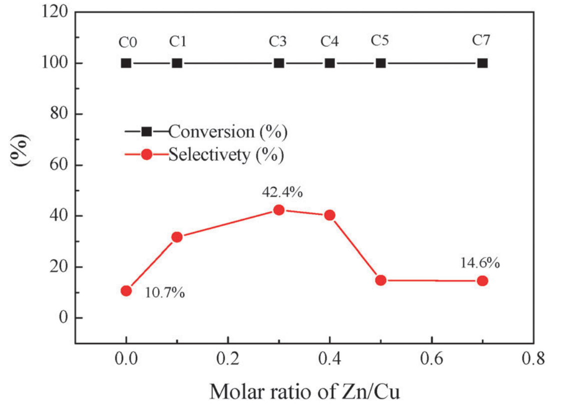

Fig. 3 The effect of Zn/Cu in Cu/ZnO/Al_2O_3 (Cat./L-p = 1 : 1) on the conversion and chemoselectivity of methyl L-phenylalaninol for the catalytic hydrogenation of methyl L-phenylalaninate at 70 °C and 3 MPa of H_2 for 5 h.

at 80 °C and 3 MPa of H_2 for 5 h and the results are shown in Fig. 3. The results show that the Cu/ZnO/Al_2O_3 and Cu/Al_2O_3 catalysts exhibit a high activity, that is, ~100% conversion of L-phenylalaninate can be obtained at this reaction condition. However, the yield of desired product (methyl L-phenylalaninol) is different for the different catalysts and is strongly related to the ZnO content in the Cu/ZnO/Al_2O_3 catalyst, because of the ZnO content affecting the Cu surface area and Cu dispersion. The results in Fig. 3 show that, the methyl L-phenylalaninol chemoselectivity (CS-nol) over the Cu/Al_2O_3 catalyst is 10.7%, and after adding ZnO in the Cu/Al_2O_3 catalyst, CS-nol is increased obviously. When using the C3 catalyst (Zn/Al = 0.3), the maximum CS-nol (42.4%) can be obtained, and upon further increasing the ZnO content in the Cu/ZnO/Al_2O_3 catalyst, CS-nol is instead decreased.

As shown in Table 2, the Cu surface area of the Cu/ZnO/Al_2O_3 catalyst is increased with the BET surface area, and the Cu dispersion is increased with the Cu surface area. Based on the BET surface area, Cu surface area and Cu dispersion of the Cu/ZnO/Al_2O_3 catalyst, we can conclude that CS-nol is increased with the Cu dispersion that is enhanced by increasing Cu surface area.

3.3.2 Effects of reaction conditions. Based on the results above, among the prepared Cu/ZnO/Al_2O_3 catalysts, the C3 catalyst is an optimized catalyst for methyl L-phenylalaninate hydrogenation to methyl L-phenylalaninol. Therefore the C3 catalyst was used as a model catalyst to investigate the effect of the reaction conditions, such as the reaction temperature, time, pressure and the Cat./L-p mass ratio on the yield of methyl L-phenylalaninol (that is the chemoselectivity to methyl L-phenylalaninol in 100% conversion of methyl L-phenylalaninate).

The influence of the reaction temperature on the yield of methyl L-phenylalaninol was investigated at 70–150 °C and 3 MPa of H_2 for 5 h and Cat./L-p = 1, and the results are shown in Fig. 4A. The results show that the yield of methyl L-phenylalaninol is increased with the reaction temperature, however, when the reaction temperature is more than 110 °C, any increase of yield is unnoticeable. Therefore, the appropriate reaction temperature is 110 °C.

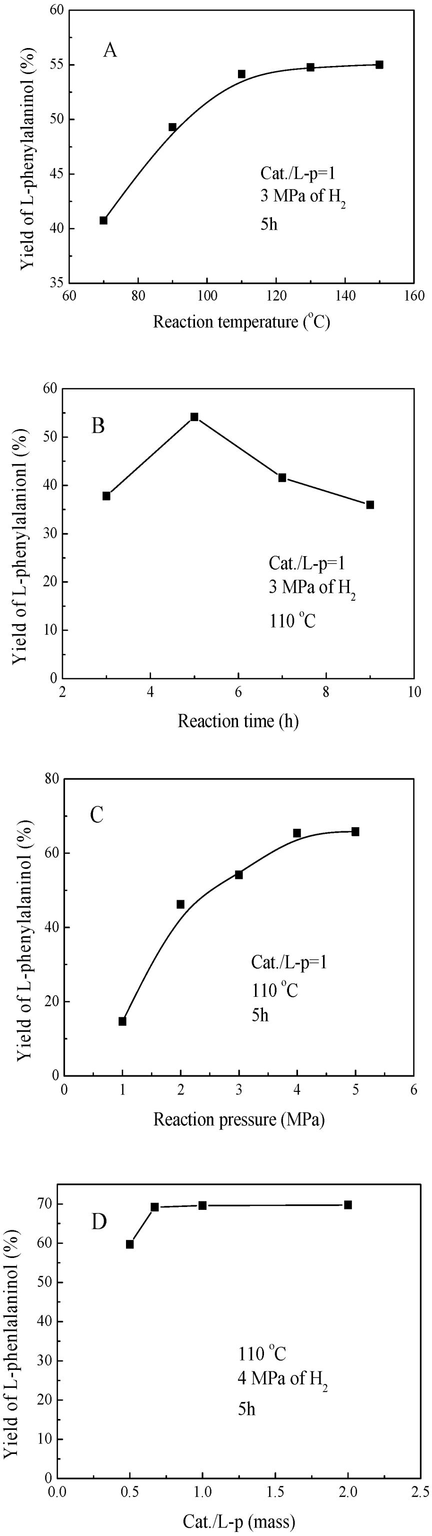

Fig. 4 Influence of reaction conditions on the yield of methyl L-phenylalaninol over the C3 catalyst: (A) temperature, (B) time, (C) pressure and (D) Cat./L-p. (Reaction conditions: (A) Cat./L-p = 1, at 3 MPa of H_2 for 5 h, (B) Cat./L-p = 1, at 110 °C and 3 MPa of H_2; (C) Cat./L-p = 1, at 110 °C for 5 h, and (D) at 110 °C and 4 MPa of H_2 for 5 h).

The influence of the reaction time on the yield of L-phenylalaninol at 110 °C and 3 MPa of H_2 and Cat./L-p = 1 is shown in Fig. 4B. It shows that with an increase in the reaction time from 3 to 5 h, the yield of methyl L-phenylalaninol is increased, and after 5 h, it is decreased. As the conversion of methyl L-phenylalaninate is ~100%, the chemoselectivity to by-products is increased with reaction time after 5 h. Therefore the appropriate reaction time is 5 h when the reaction is operated at 110 °C.

The effect of the hydrogen pressure on the catalytic hydrogenation of L-phenylalanate was studied at 110 °C and Cat./L-p = 1 for 5 h, and the results are shown in Fig. 4C. It is observed that the yield of methyl L-phenylalaninol is increased with H_2 pressure, and when H_2 pressure is more than 4 MPa, the yield almost remains constant. Hence the appropriate reaction pressure is 4 MPa.

Fig. 4D shows the effect of the catalyst content (Cat./L-p) on the yield of methyl L-phenylalaninol. We can see that when Cat./L-p is less than 1.0 : 1.5, the yield of methyl L-phenylalaninol is increased with increasing the catalyst amount; when Cat./L-p is more than 1.0 : 1.5, the yield of methyl L-phenylalaninol is hardly changed with the catalyst amount.

Based on the results mentioned above, the more optimal reaction conditions for the selective hydrogenation of methyl L-phenylalaninate to methyl L-phenylalaninol over the $Cu/ZnO/Al_2O_3$ catalyst can be determined, which are 110 °C, 4 MPa of H_2, 5 h and Cat./L-p = 1.0 : 1.5. At such reaction conditions, the yield of methyl L-phenylalaninol can reach 69.2%. The *ee* value of the product is 99.84% obtained by HPLC (with the separation column of Chiralcel OD, 250 × 4.6 mm) after the chiral amine of methyl phenylalaninol was protected by benzyl chloroformate.[53] The ^{1}H NMR spectrum of methyl L-phenylalaninol was obtained on a Bruker AVANCE-III 500. ^{1}HNMR($CDCl_3$): 7.16–7.29 (5H, m, Ph-H), 3.41–3.66 (2H, m, $-CH_2-O-$), 3 3.15–3.20 (1H, m, $CHNH_2$), 2.51–2.82 (2H, m, CH_2 Ph).

3.3.3 Turnover frequency of catalyst for hydrogenation of methyl L-phenylalaninate. Turnover frequencies (TOFs) for product[54] and average reaction rates of $Cu/ZnO/Al_2O_3$ catalysts for the selective hydrogenation of methyl L-phenylalaninate to methyl L-phenylalaninol are shown in Table 3. It can be seen that the C3 catalyst exhibits the highest yield (69.2%) and the largest reaction rate (1.16 mmol g_{cat}^{-1} h^{-1}), because of C3 possessing the most active sites per gram of catalyst. For TOF, $Cu/ZnO/Al_2O_3$ is higher than Cu/Al_2O_3, indicating that the presence of Zn enhances the catalytic activity of the Cu sites. However, the TOF of C7 is higher than that of C3, which gives us enlightenment that the higher effective active sites can be designed and prepared by highly loading Zn to modify Cu sites to form more surface defects of metallic Cu (such as step, kink, edge, and so on), because these defect Cu sites exhibit only catalytic activity. Additionally, the higher effective $Cu/ZnO/Al_2O_3$ catalyst can be prepared by increasing the Cu surface area of $Cu/ZnO/Al_2O_3$ because the larger the surface area of Cu, the more active sites of Cu and the higher the catalytic activity.

Table 3 TOFs, reaction rates and product yields for hydrogenation of methyl L-phenylalaninate over $Cu/ZnO/Al_2O_3$ catalysts[a]

Catalyst	Yield of methyl L-phenylalaninol (%)	Number of active sites ($\times 10^{20}$ g_{cat}^{-1})	TOF (h^{-1})[b]	Average rate (mmol g_{cat}^{-1} h^{-1})[c]
C0	12.8	13.1	0.099	0.21
C1	53.2	13.0	0.413	0.89
C3	69.2	15.8	0.441	1.16
C4	61.9	12.7	0.491	1.04
C5	31.0	5.12	0.610	0.52
C7	45.3	4.82	0.947	0.76

[a] Reaction conditions: 1.5 g methyl L-phenylalaninate, 1.0 g $Cu/ZnO/Al_2O_3$ catalyst (Cat./L-p = 1.0 : 1.5), 110 °C, 4 MPa of H_2, 5 h. [b] Turnover frequencies for methyl L-phenylalaninol formed, mol product per Cu per hour at 110 °C.[54] [c] The average reaction rate for 5 h.

4 Conclusions

In summary, the $Cu/ZnO/Al_2O_3$ catalyst that showed the highest catalytic activity and *ee* selectivity towards the product for the hydrogenolysis of methyl L-phenylalaninate to methyl L-phenylalaninol was designed and prepared by a co-precipitation method. Metallic copper plays the role of the active site for the hydrogenation reactions, and ZnO can promote the dispersion of copper (oxide) and enhance the reducibility of the copper oxide phase. The appropriate molar ratio of Zn/Cu should be ~0.3.

The $Cu/ZnO/Al_2O_3$ catalyst with a Cu/Zn/Al molar ratio of 1.0 : 0.3 : 1.0 shows the highest activity and *ee* selectivity to methyl L-phenylalaninol. Over this catalyst, methyl L-phenylalaninate was hydrogenated at 110 °C and 4 MPa of H_2 for 5 h, at which the yield of methyl L-phenylalaninol can reach 69.2%, and its *ee* = 99.84%. Since the $Cu/ZnO/Al_2O_3$ catalyst is very cheap and easily prepared for the selective hydrogenation, further investigations regarding the catalytic reaction mechanism and improvement of the chemoselectivity are in progress and will be reported in due course.

Acknowledgements

We would like to acknowledge the financial support from the National Basic Research Program of China (2010CB732300), and the ''Shu Guang'' Project (10GG23) and Leading Academic Discipline Project (J51503) of Shanghai Municipal Education Commission and Shanghai Education Development Foundation, and The School to Introduce Talents Project (YJ2011-46).

References

1 E. J. Corey, S. Shibata and R. K. Bakashi, *J. Org. Chem.*, 1988, **53**, 2861.
2 C. B. Li, J. Zhang, P. Y. Zhao and M. Lu, *J. Tianjin Univ.*, 2004, **37**(10), 923.
3 S. J. Lv, R. Jiang, H. Y. Zhou, Y. Zheng and H. X. Fu, *Chin. J. Mol. Catal.*, 1995, **9**(5), 358.
4 J. M. Andres, Y. Martin, R. Pedrosa and A. P. Encabo, *Tetrahedron*, 1997, **53**, 3787.
5 D. Pini and A. Mastantuono, *Tetrahedron: Asymmetry*, 1994, **5**, 1875.
6 G. J. Lee, T. H. Kim and J. N. Kim, *Tetrahedron: Asymmetry*, 2002, **13**, 9.

7 M. Kawai, Y. Omori and H. Yamamura, *Tetrahedron: Asymmetry*, 1992, **3**, 1019.
8 J. R. Luly, J. J. Plattner, H. Stein, N. Yi, J. Soderquist, P. A. Marcotte, H. D. Kleinert and T. J. Perun, *Biochem. Biophys. Res. Commun.*, 1987, **143**, 44.
9 J. M. Cassal and A. Fuerst, *Helv. Chim. Acta*, 1976, **59**, 1917.
10 C. F. Stanfield, J. E. Parker and P. Kanellis, *J. Org. Chem.*, 1981, **46**, 4799.
11 D. A. Dickman and A. I. Meyers, *Org. Synth.*, 2001, **7**, 530.
12 Q. Hua, J. Z. Lin and Q. Jiang, *Chem. Reagents*, 1993, **15**, 123.
13 B. Bai, X. Y. Li, Y. Li and H. J. Zhu, *Bioorg. Med. Chem. Lett.*, 2011, **21**, 2302.
14 Z. X. Shen, Y. H. Li, H. B. Qin and Y. W. Zhang, *Chem. Reagants*, 2004, **15**, 23.
15 H. H. He, D. C. Gong and P. Wei, *Chem. Reagants*, 2005, **27**(2), 115.
16 C. H. Zhang, N. F. Yang and L. W. Yang, *Chin. J. Org. Chem.*, 2004, **24**, 343.
17 C. F. Gan, R. Feng, J. C. Fan and J. G. Cui, *Chem. World*, 2007, **9**, 538.
18 Z. X. Wang and Y. Q. Fu, *J. Luoyang Normal Univ.*, 2007, **5**, 69.
19 F. Massimo, P. Andrea and T. Maurizio, *Tetrahedron Lett.*, 1999, **40**, 4395.
20 D. C. Gong, P. Wei, H. H. He, H. Zhou and P. K. Ouyang, *Chin. Fine Chem.*, 2005, **22**(5), 384.
21 Y. Z. Li, C. X. Guo, X. Y. Lu, L. C. Shen and H. M. Huang, *J. Jilin Univ., Earth Sci. Ed.*, 1998, **1**, 85.
22 S. Narasimhan, S. Madhavan and K. G. Prasad, *J. Org. Chem.*, 1995, **60**, 5314.
23 J. M. Herbert, A. T. Hewson and J. E. Peace, *Synth. Commun.*, 1998, **28**, 823.
24 T. Kashiwagi, S. Kotani, M. Sugiura and M. Nakajima, *Tetrahedron*, 2011, **67**, 531.
25 A. Abiko and S. Masamune, *Tetrahedron Lett.*, 1992, **33**, 5517.
26 M. Studer, S. Burkhardt and H. U. Blaser, *Adv. Synth. Catal.*, 2001, **343**, 802.
27 G. Ovakimim, M. Kuna and P. A. Levene, *J. Biol. Chem.*, 1940, **135**, 91.
28 W. Kuriyama, Y. Ino, O. Ogata, N. Sayo and T. Saito, *Adv. Synth. Catal.*, 2010, **352**, 92.
29 D. S. Brands, E. K. Poels and A. Bliek, *Appl. Catal., A*, 1999, **184**, 279.
30 V. D. Kumari, M. Subrahmanyam, A. Ratnamala, D. Venugopal, B. Srinivas, M. V. P. Sharma, S. S. Madhavendra, B. Bikshapathi, K. Venkateswarlu, T. Krishnudu, K. B. S. Prasad and K. V. Raghavan, *Catal. Commun.*, 2002, **3**, 417.
31 U. Costantino, F. Marmottini, M. Sisani, T. Montanari, G. Ramis, G. Busca, M. Turco and G. Bagnasco, *Solid State Ionics*, 2005, **176**, 2917.
32 A. Indarto, D. R. Yang, J. Palgunadi, J. W. Choi, H. Lee and H. K. Song, *Chem. Eng. Process.*, 2008, **47**, 780.
33 M. Behrens, D. Brennecke, F. Girgsdies, S. Kiβner, A. Trunschke, N. Nasrudin, S. Zakaria, N. F. Idris, S. B. A. Hamid, B. Kniep, R. Fischer, W. Busser, M. Muhler and R. Schlögl, *Appl. Catal., A*, 2011, **392**, 93.
34 H. F. Wang, L. G. Chen, G. Y. Bai, D. Z. Luan, Y. Li, X. L. Yan, Y. C. Zhang and J. D. Xing, *Catal. Commun.*, 2007, **8**, 145.
35 Y. H. Feng, H. B. Yin, A. L. Wang, L. Q. Shen, L. B. Yu and T. S. Jiang, *Chem. Eng. J.*, 2011, **168**, 403.
36 Z. M. Zhou, X. Li, T. Y. Zeng, W. B. Hong, Z. M. Cheng and W. K. Yuan, *Chin. J. Chem. Eng.*, 2010, **18**(3), 384.
37 F. T. van de Scheur, B. van der Linden, M. C. M. Hazeleger, J. G. Nazloomian and L. H. Staal, *Appl. Catal., A*, 1994, **111**, 63.
38 P. Claus, M. Lucas, B. Lücke, T. Berndt and P. Birke, *Appl. Catal., A*, 1991, **79**, 1.
39 J. C. Frost, *Nature*, 1988, **334**, 577.
40 D. S. Brands, E. K. Poels and A. Bliek, *Stud. Surf. Sci. Catal.*, 1996, **101**, 1085.
41 D. S. Brands, E. K. Poels, T. A. Krieger, O. V. Makarova, C. Weber, S. Veer and A. Bliek, *Catal. Lett.*, 1996, **36**, 175.
42 T. M. Yurieva, L. M. Plyasova, O. V. Makarova and T. A. Krieger, *J. Mol. Catal. A: Chem.*, 1996, **113**, 455.
43 Y. Kawamura, K. Yamamoto, N. Ogura, T. Katsumata and A. Igarashi, *J. Power Sources*, 2005, **150**, 20.
44 Z. L. Yuan, L. N. Wang, J. H. Wang, S. X. Xia, P. Chen, Z. Y. Hou and X. M. Zheng, *Appl. Catal., B*, 2011, **101**, 431.
45 C. J. G. Van Der Grift, A. F. H. Wielers, B. P. J. Jogh, J. V. Beunum, M. De Boer, M. V. Helder and J. W. Geus, *J. Catal.*, 1991, **131**, 178.
46 X. M. Guo, D. S. Mao, G. Z. Lu, S. Wang and G. S. Wu, *J. Catal.*, 2010, **271**, 178.
47 I. M. Cabrera, M. L. Granados and J. L. G. Fierro, *J. Catal.*, 2002, **210**, 273.
48 M. F. Luo, P. Fang, M. He and Y. L. Xie, *J. Mol. Catal. A: Chem.*, 2005, **239**, 243.
49 Z. Li, H. Y. Zheng and K. C. Xie, *Chin. J. Catal.*, 2008, **29**(5), 431.
50 G. Z. Lu and R. Wang, *Chin. J. Catal.*, 1991, **12**, 83.
51 F. Arena, K. Barbera, G. Italiano, G. Bonura, L. Spadaro and F. Frusteri, *J. Catal.*, 2007, **249**, 185.
52 Y. P. Zhang, J. H. Fei, Y. M. Yu and X. M. Zheng, *Energy Convers. Manage.*, 2006, **47**, 3360.
53 J. Clariana, S. G. Granda, V. Gotor, A. G. Fernandez, A. Luna, M. M. Manas and A. Vallribera, *Tetrahedron: Asymmetry*, 2007, **48**, 8323.
54 S. X. Xia, R. F. Nie, X. Y. Lu, L. N. Wang, P. Chen and Z. Y. Hou, *J. Catal.*, 2012, **296**, 1.